International Journal of Heat and Technology
Vol. 43, No. 6, December, 2025, pp. 2226-2236
Journal homepage: http://iieta.org/journals/ijht

Techno-Economic Feasibility Assessment of Energy Technologies Through the Integration of Thermodynamics and Life-Cycle Cost Analysis

Lipeng Wang

Shijiazhuang University of Applied Technology, Shijiazhuang 050081, China

Corresponding Author Email: 2003100270@sjzpt.edu.cn

https://doi.org/10.18280/ijht.430621

Received: 20 April 2025
Revised: 12 October 2025
Accepted: 29 October 2025
Available online: 31 December 2025

Keywords:
thermodynamics, life-cycle cost analysis, exergy analysis, MEDCC, energy system design optimization, synergistic evaluation

ABSTRACT

As the global energy transition enters a critical phase driven by carbon neutrality targets and the large-scale penetration of renewable energy, energy systems are evolving toward complex, multi-energy complementary configurations. This transformation requires the coordinated optimization of efficiency, cost, and environmental performance. However, the traditional disciplinary separation between thermodynamic analysis and economic evaluation, together with the limitations of existing integrated approaches, constrains their ability to support accurate and mechanism-informed design decisions. This study proposes a unified theoretical framework based on the synchronous mapping of thermodynamic value degradation and economic cost formation. By reformulating life-cycle cost analysis as a dynamic tracking process accompanying exergy flow evolution, the proposed framework overcomes the mechanistic disconnection and static limitations of conventional evaluation methods. An exergy cost formation rate equation and the marginal exergy destruction cost coefficient (MEDCC) are developed to establish a continuously differentiable quantitative mapping from thermodynamic parameters to full life-cycle economic performance. Furthermore, environmental exergy loss quantification and carbon cost internalization are incorporated to construct a three-dimensional synergistic evaluation system encompassing thermodynamic, economic, and environmental dimensions. Case studies of representative energy systems demonstrate that the proposed framework can accurately identify the coupling between thermodynamic hotspots and economic improvement hotspots, reveal discrepancies between thermodynamic optima and economic optima, and derive scientifically grounded optimization sequences. This research establishes a unified evaluation theory rooted in both thermodynamics and economics, overcomes the assessment bottlenecks of complex energy systems under high renewable energy penetration, and provides an efficient decision-support tool for multi-dimensional synergistic energy system design and optimization, with significant theoretical and practical implications.

1. INTRODUCTION

The global energy transition has entered a critical stage driven by carbon neutrality targets and the high penetration of renewable energy [1, 2]. Energy systems are evolving from traditional single-supply modes toward complex synergistic modes with multi-energy complementarity [3]. In this transformation process, energy system design is required to simultaneously satisfy the three-dimensional synergistic requirements of efficiency improvement, cost optimization, and environmental friendliness. However, the separation between thermodynamic performance evaluation and economic feasibility assessment in traditional evaluation systems has become insufficient to support accurate design decisions for complex energy technologies [4, 5]. Classical evaluation methods either focus on diagnosing thermodynamic irreversibility while neglecting economic costs [6], or emphasize cost accounting while lacking thermodynamic mechanism support [7], and thus fail to reveal the intrinsic relationship between energy quality degradation and economic cost generation. Under this background, it is urgently necessary to establish an integrated evaluation theory that deeply couples thermodynamic characteristics with economic costs, providing scientific support for energy system design optimization oriented toward multi-dimensional synergy. Accordingly, the core scientific question of this study is clearly defined: how to construct a synchronous mapping mechanism between thermodynamic irreversible processes and full life-cycle cost generation, to achieve a continuously differentiable quantitative relationship from thermodynamic parameters to economic indicators, thereby overcoming the inherent limitations of traditional evaluation methods in design guidance.

The cross-integration of thermodynamic evaluation and economic evaluation is the core direction for addressing the above problem. Relevant research fields have formed three representative research paradigms, but their inherent deficiencies have not yet been fundamentally resolved.

Classical exergy analysis takes energy quality as its core and can accurately identify thermodynamic performance weaknesses of systems by quantifying state exergy, exergy destruction, and exergy efficiency [8-10]. However, this paradigm remains at the level of physical property diagnosis and does not establish a quantitative connection with economic costs, making it unable to directly support design decisions related to cost optimization. As an early integration attempt, exergoeconomics achieves a preliminary combination of exergy and cost, but existing studies are mostly limited to instantaneous cost allocation at the component level and have not been extended to the full life-cycle time scale. In addition, the integration mechanism between capital cost and thermodynamic parameters lacks flexibility [11, 12], making it difficult to reflect the dynamic evolution relationship between cost and exergy flows during system operation. Traditional life-cycle cost analysis can cover economic accounting over the full life cycle of a system, but it mostly adopts a black-box evaluation logic, in which the identification of cost-driving factors is detached from the fundamental support of thermodynamic irreversibility [13, 14], leading to optimization recommendations that may conflict with improvements in system thermodynamic performance. In summary, existing studies have not established a deeply coupled mechanism between thermodynamic value degradation and economic cost generation, and generally exhibit three core gaps: the lack of a full life-cycle perspective, the disconnection of quantitative mapping between thermodynamics and economics, and insufficient design guidance capability. These gaps urgently require breakthroughs through theoretical and methodological innovation.

In response to the above research gaps, this study conducts systematic innovation from three dimensions: theory, methodology, and application. The main contributions are as follows. At the theoretical framework level, the concept of synchronous mapping between thermodynamic value degradation and economic cost generation is proposed for the first time, breaking the disciplinary separation between traditional thermodynamic evaluation and economic evaluation. Static life-cycle cost analysis is transformed into a dynamic cost tracking process accompanying exergy flow evolution, establishing a unified theoretical foundation rooted in both thermodynamics and economics. At the methodological level, an exergy cost formation rate equation and an MEDCC are established, realizing a continuously differentiable quantitative mapping from thermodynamic parameters to full life-cycle economic indicators, and providing quantitative tools for accurately diagnosing economic improvement hotspots. At the application level, a thermodynamic decision-support system with both performance evaluation and design optimization guidance functions is developed. This system not only quantifies the thermodynamic–economic comprehensive performance of energy systems, but also accurately identifies key stages and priority sequences for cost optimization, providing direct technical support for cost-oriented energy technology design.

The remainder of this paper is organized as follows. Section 2 constructs the core theoretical framework of the synchronous mapping model and clarifies system boundary definitions, basic thermodynamic models, and the mathematical formulations of the core innovative modules. Section 3 conducts application validation using representative energy systems as case studies, verifying the effectiveness of the model through coupled analysis of thermodynamic and economic data. Section 4 discusses the advantages, limitations, and key implications of the proposed method for energy system design. Section 5 summarizes the main conclusions and outlines future research directions.

2. THEORETICAL FRAMEWORK

2.1 System boundaries and basic definitions

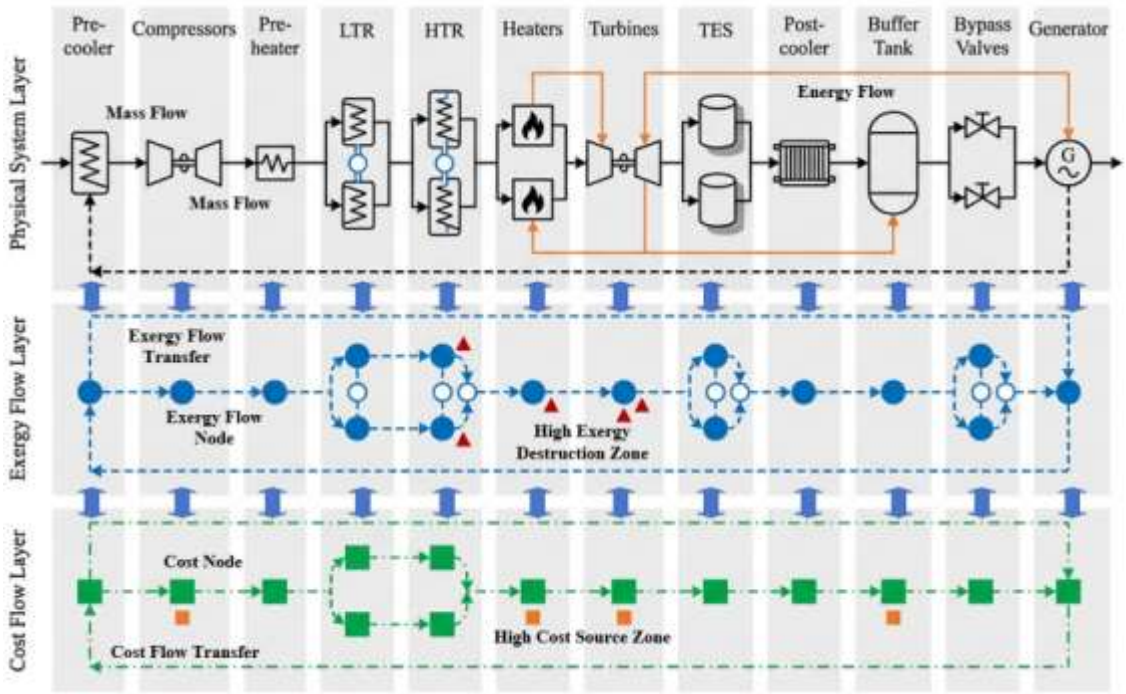

Figure 1. Schematic diagram of the three-in-one representation of an energy system: "physical system – exergy flow network – cost network"

The precise definition of system boundaries is a prerequisite for constructing the synchronous mapping model, requiring clear identification of both the physical boundary of the research object and the full life-cycle time boundary [15]. The physical boundary is centered on the core conversion and transmission components of the energy system and includes all units involved in energy conversion, exergy flow transfer, and cost circulation [16]. The time boundary covers the entire life-cycle stages from planning, design, construction, operation, and maintenance to decommissioning [17]. To achieve dynamic matching between cost and exergy flows, discrete full life-cycle costs need to be converted into continuous cost flow rates. The core conversion formula is the annualization formula of life-cycle cost: $\dot{Z}_k = Z_k \cdot CRF$, where Z_k is the total life-cycle cost of component k, $\dot{Z}_k$ is the annualized cost flow rate of component k, and CRF is the capital recovery factor, expressed as:

$$CRF = \frac{i(1+i)^n}{(1+i)^n - 1} \tag{1}$$

where, i is the reference discount rate and n is the service life of the component. Based on the boundary definitions, a three-in-one representation system of "physical system–exergy flow network–cost network" is established by drawing system flow diagrams and exergy Grassmann diagrams. The system flow diagram presents the interactions of material and energy among components, while the exergy Grassmann diagram accurately indicates exergy flow inputs and outputs at each node, the locations of exergy destruction, and the inlets and outlets of cost flows. Combined with the annualized cost flow rate formula, precise correspondence among physical structure, energy quality evolution, and economic cost circulation is achieved. Figure 1 takes an extended supercritical CO_2 Brayton cycle model as an example to construct a vertically layered three-level network structure, clearly showing the one-to-one correspondence and coupling mechanisms among the physical system, the exergy flow network, and the cost network.

2.2 Physical basis: Classical exergy analysis model

Classical exergy analysis is the physical basis of thermodynamic–economic synchronous mapping. Its core lies in quantifying the available quality of energy and the quality degradation caused by irreversible processes. The key parameters and governing equations are given as follows [18]. State exergy is a quantitative indicator of energy availability and is divided into physical exergy and chemical exergy. Physical exergy reflects the available energy resulting from the deviation of system temperature and pressure from the environmental state (T_0, p_0), and is calculated as: $E_{ex,ph} = (H - H_0) - T_0(S - S_0)$, where H and S are the enthalpy and entropy of the system, respectively, and H_0 and S_0 are the enthalpy and entropy at the environmental state. Chemical exergy reflects the available energy resulting from the deviation of system composition from the environmental composition. For a single ideal gas component, the simplified calculation formula is:

$$E_{ex,ch} = RT_0 \ln \frac{y_0}{y} \tag{2}$$

where, R is the gas constant, and y and y_0 are the mole fractions of the component in the system and in the environment, respectively. Exergy destruction is the direct representation of irreversible processes and is obtained through the exergy balance equation. The general exergy balance equation for the system and each component is:

$$\sum E_{ex,in} + \sum W_{in} = \sum E_{ex,out} + \sum E_{ex,dest} \tag{3}$$

where, $E_{ex,in}$ and $E_{ex,out}$ are the input and output exergy flows, respectively, W_{in} is the useful work input from the surroundings, and $E_{ex,dest}$ is the exergy destruction caused by irreversible processes. Exergy efficiency reflects the utilization efficiency of exergy and is defined as the ratio of effective output exergy to total input exergy:

$$\eta_{ex} = \frac{\sum F_{ex,out,eff}}{\sum F_{ex,in,total}} \tag{4}$$

By solving the exergy balance equations of each component, the exergy flow transfer paths and the distribution pattern of exergy destruction throughout the entire system can be quantified. Combined with the quantified results of state exergy and exergy efficiency, this provides a clear physical carrier and evolution path for the subsequent dynamic tracking of economic costs.

2.3 Core innovation: Exergy cost formation rate model and full life-cycle cost tracking

2.3.1 Core definitions and tracking axioms

The core of the exergy cost formation rate model is to establish a dynamic binding relationship between cost flows and exergy flows. For this purpose, the exergy cost flow rate is first defined as the core quantitative indicator. The exergy cost flow rate, $\dot{C}_{ex}$, represents the economic cost flow accompanying exergy transfer per unit time. Its physical and economic implication lies in transforming discrete full life-cycle costs into dynamic variables that evolve synchronously with continuous exergy flows, thereby achieving time-scale matching between the cost transfer process and the exergy flow evolution process. The introduction of this indicator overcomes the limitations of traditional static cost allocation and provides a quantitative carrier for tracking the dynamic circulation of costs among system components. Its unit is €/s to ensure dimensional consistency with the exergy flow rate. Figure 2 presents the core logic of dynamic exergy cost tracking through a composite structure with upper and lower layers and intermediate processes, and accurately maps the supporting nodes and operating mechanisms of the three major cost tracking axioms.

Based on the physical nature of exergy and the economic attributes of full life-cycle costs, three cost tracking axioms are proposed as the logical foundation for dynamic cost tracking. Axiom 1 is the transferability axiom, which clarifies that economic costs strictly accompany exergy flow transfer, and the transfer path of exergy flow is the tracking path of cost. This axiom establishes the physical dependency of cost transfer and avoids the introduction of subjective allocation rules in traditional cost allocation. Axiom 2 is the exergy destruction bearing axiom, which stipulates that the economic cost corresponding to exergy destruction generated by irreversible processes is fully borne by the product exergy output of the system.

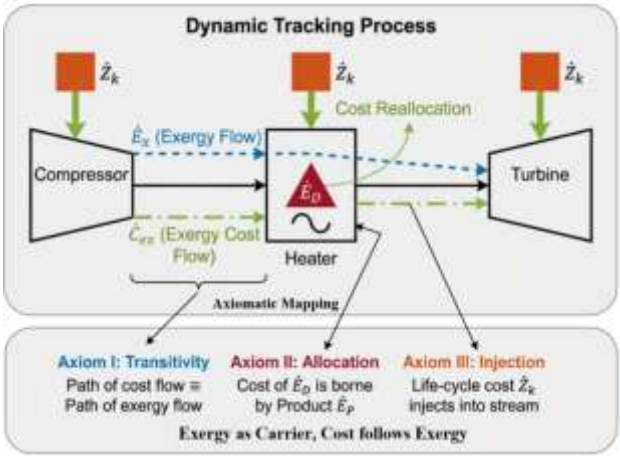

Figure 2. Schematic diagram of dynamic exergy cost tracking logic and mapping of the three axioms

The core rationale is that exergy destruction represents irreversible degradation of energy quality and essentially corresponds to a loss of resource value, which should be carried by the final product. Axiom 3 is the cost source injection axiom, which indicates that the full life-cycle cost of each component, as a new cost source, is uniformly injected into its output exergy flow and participates in subsequent transfer. This setting realizes the organic integration of full life-cycle costs, including capital cost and operating cost, with exergy flows, and resolves the rigid integration of capital cost and thermodynamic parameters in traditional exergoeconomics. The three axioms support each other and jointly construct a dynamic tracking logic system of "exergy flow as carrier, cost follows exergy, losses borne by products, and cost source injection," providing a solid theoretical foundation for subsequent mathematical modeling.

2.3.2 Mathematical modeling and solution algorithm

Based on the above definitions and axioms, a general component-level exergy cost balance equation is established to realize the quantitative coupling between cost flows and exergy flows. For an arbitrary component k, the exergy cost balance equation is:

$$\sum \dot{C}_{ex,out} = \sum \dot{C}_{ex,in} + \dot{Z}_k \tag{5}$$

where, $\sum \dot{C}_{ex,in}$ and $\sum \dot{C}_{ex,out}$ are the total exergy cost flow rates corresponding to the input and output exergy flows of the component, respectively; $\dot{Z}_k$ is the annualized full life-cycle cost flow rate of component k, which is the key parameter linking full life-cycle cost and dynamic cost tracking. The calculation of $\dot{Z}_k$ covers the full scope of capital expenditure (CAPEX) and operating expenditure (OPEX). CAPEX includes one-time costs such as initial investment and installation and commissioning, while OPEX covers periodic costs such as operation and maintenance, fuel consumption, and decommissioning and disposal. The total full life-cycle cost (*TotalLCC*) Z_k is converted into an annualized cost flow rate through the capital recovery factor CRF, namely $\dot{Z}_k = Z_k \cdot CRF$, where the expression of CRF is:

$$CRF = \frac{i(1+i)^n}{(1+i)^{n-1}} \tag{6}$$

where, i is the reference discount rate and n is the service life of the component. In terms of quantitative boundaries, CAPEX is aggregated at the time of component commissioning, while OPEX is accounted for based on the actual annual occurrence, ensuring complete coverage and accurate conversion of full life-cycle costs.

The solution of the exergy cost flow rate takes the results of classical exergy analysis as inputs and adopts an iterative algorithm to achieve global solution of cost flows for the entire system. The core procedure consists of three steps. First, the unit exergy cost of fuel c_f is determined as the initial reference for cost flow calculation. c_f is determined based on the ratio of the fuel market price to the fuel exergy value:

$$c_f = \frac{P_t}{E_{ex,f}} \tag{7}$$

where, P_f is the market price per unit mass of fuel, and $E_{ex,f}$ is the exergy value per unit mass of fuel, ensuring that fuel cost is directly linked to fuel energy quality. Second, constrained by the exergy balance results of each component, the exergy cost balance equations are solved iteratively. Starting from the fuel input component, the input exergy cost flow rate of each component is calculated sequentially, and the output exergy cost flow rate is obtained by combining $\dot{Z}_k$, thereby yielding the unit exergy cost of component output c_{ex}. For components with multiple inputs and outputs, the cost allocation ratio of each output exergy is determined based on the exergy flow distribution proportion. Iteration continues until the unit exergy costs of all components in the system converge, and the final unit exergy cost of the system product c_p is obtained.

To achieve consistency between thermodynamic–economic indicators and commonly used economic evaluation indicators in the energy industry, a direct conversion relationship between c_p and the levelized cost of energy (LCOE) is established. Considering the annual operating time of the system τ and the annual product energy output Q_{annual}, the conversion formula between the product unit exergy cost c_p and LCOE is:

$$LCOE = c_p \cdot \frac{E_{exp,annual}}{Q_{annual}} \tag{8}$$

where, $E_{ex,p,annual}$ is the total annual product exergy output of the system. This conversion relationship transforms exergy-based thermodynamic–economic indicators into LCOE, which is widely recognized in the energy industry, ensuring comparability of evaluation results and enhancing the engineering applicability of the model. Through the above mathematical modeling and solution process, full-chain dynamic tracking from fuel cost and full life-cycle cost to product cost is realized, as well as quantitative mapping from thermodynamic parameters to economic indicators. Figure 3 presents the complete calculation procedure of MEDCC using the model perturbation method.

2.4 Diagnostic and optimization tool: MEDCC

MEDCC is the core diagnostic indicator linking thermodynamic improvement and economic optimization. Its definition originates from the marginal coupling relationship between exergy destruction and the *TotalLCC* of the system. The mathematical expression is:

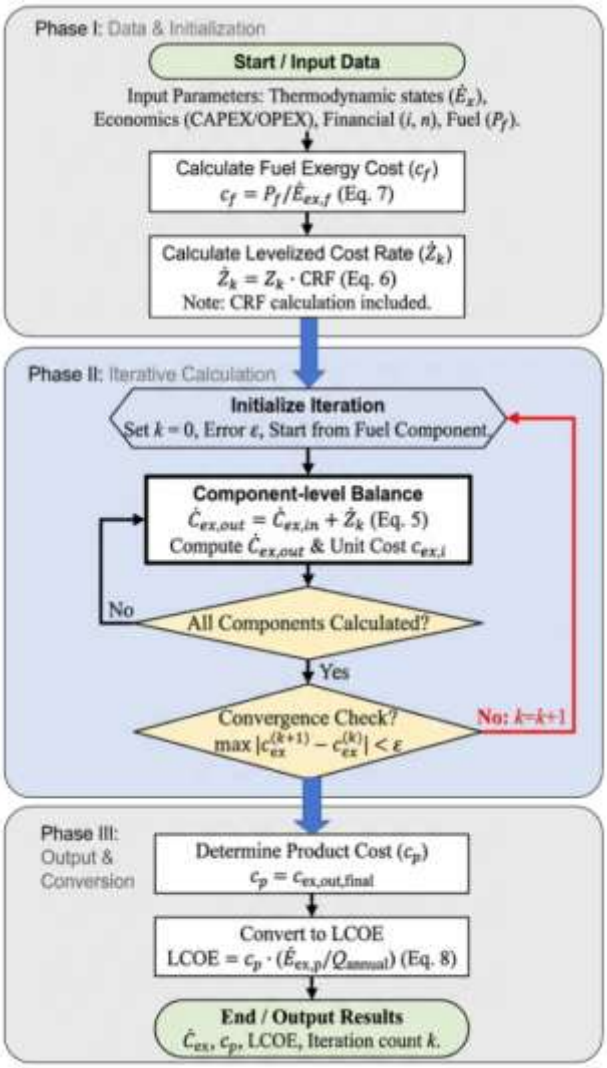

Figure 3. Flowchart of the iterative solution algorithm for exergy cost flow rate

$$MEDCC_k = \frac{\partial(TotalLCC)}{\partial(Ex_{dest,k})} \tag{9}$$

where, $Ex_{dest,k}$ is the exergy destruction of component k. The partial derivative constraint ensures that the independent impact of exergy destruction variation of a single component on the total cost is accurately captured. The core value of this definition lies in overcoming the limitation of traditional exergy destruction analysis that "only evaluates magnitude but not cost," and realizing the economic value quantification of thermodynamic losses.

The physical–economic significance of *MEDCC* can be interpreted from two dimensions. From the physical dimension, it quantifies the dynamic response relationship between variations in component exergy destruction and changes in the total system cost, reflecting the economic transmission effect of thermodynamic irreversible processes. From the economic dimension, its value directly represents the "marginal change in *TotalLCC* induced by reducing a unit of exergy destruction." When *MEDCC* is positive, it indicates that reducing exergy destruction will lead to a decrease in total cost and has economic improvement value, and the larger the absolute value, the more significant the economic benefit per unit exergy destruction improvement. When *MEDCC* is negative or approaches zero, it indicates that reducing exergy destruction may lead to cost increases or no economic benefit, and the optimization priority is low. This characteristic makes *MEDCC* a key basis for identifying economic improvement hotspots, effectively distinguishing between "thermodynamic hotspots" and "economic improvement hotspots," and providing a quantitative scale for precise optimization decisions.

The calculation of *MEDCC* adopts the model perturbation method. The core idea is to induce changes in exergy destruction by applying small perturbations to key thermodynamic parameters of components, while synchronously tracking the response of the *TotalLCC* of the system, and finally obtaining the coefficient value through numerical solution of the partial derivative. This method avoids the mathematical complexity of direct differentiation and is more suitable for the nonlinear characteristics of engineering systems, with a clear engineering feasibility in its calculation procedure.

The selection of perturbation parameters follows the principle of "relevance priority," giving priority to core thermodynamic parameters directly related to component exergy destruction, such as heat exchanger effectiveness, turbine expansion efficiency, and reactor reaction temperature, ensuring that parameter perturbations can directly and significantly induce changes in exergy destruction. The determination of perturbation magnitude needs to balance computational accuracy and numerical stability. Typically, 1%–5% of the baseline parameter value is selected as a small perturbation magnitude: excessively large magnitudes may cause system characteristics to deviate from the linear region and introduce nonlinear errors, while excessively small magnitudes may be masked by numerical noise, reducing result reliability. Error control is achieved through bidirectional perturbation and iterative verification. Forward and backward perturbations are applied to the same parameter, and the deviation between the two MEDCC results is calculated. If the deviation exceeds a threshold, the perturbation magnitude is adjusted and recalculated. At the same time, convergence of results under different perturbation sequences is ensured through multiple iterative optimizations.

The specific calculation steps are as follows. First, the baseline thermodynamic parameters, baseline exergy destruction, and baseline *TotalLCC* of each component are determined. Second, a small perturbation is applied to the key parameter of the target component, and the component exergy destruction $Ex_{dest,k}$ and the *TotalLCC* of the system are recalculated. Finally, the partial derivative is approximated based on the differences before and after perturbation:

$$MEDCC_k \approx \frac{\Delta Total\ LCC}{\Delta Ex_{dest,k}} \tag{10}$$

This method realizes efficient calculation of MEDCC through numerical approximation and provides accurate quantitative support for the formulation of subsequent optimization sequences.

2.5 Framework extension: Environmental exergy destruction and carbon cost internalization

To achieve three-dimensional synergistic evaluation of efficiency, cost, and environment, it is necessary to incorporate the environmental dimension into the synchronous mapping framework. The core lies in the quantification of

environmental exergy destruction and the internalization of carbon cost, so that environmental impacts are transformed into quantitative indicators that can be directly coupled with thermodynamic and economic costs. In traditional evaluations, the separation of environmental impacts from thermodynamic and economic analyses may cause optimization decisions to ignore environmental costs. The extension of this framework realizes the fundamental integration of the three while maintaining the consistency of the theoretical system.

The core of environmental exergy destruction quantification is to convert the environmental impact of pollutant emissions into "virtual environmental exergy destruction" and to establish a quantitative relationship with pollutant emissions. Taking an environmental reference state (such as the standard atmospheric environment or a reference ecosystem state) as a benchmark, pollutant emissions disrupt the equilibrium state of the environmental system, leading to a loss of available energy in the ecosystem. This loss constitutes environmental exergy destruction. For typical pollutants such as CO_2 and SO_2, based on the definition of environmental exergy, the quantitative expression can be written as: $Ex_{env,m} = m \cdot e_{env,m}$, where m is the pollutant emission amount and $e_{env,m}$ is the environmental exergy destruction coefficient per unit mass of pollutant. This coefficient is determined through thermodynamic analysis of environmental systems and reflects the degree to which pollutants damage environmental available energy. Through this transformation, environmental impacts are incorporated into the exergy flow evolution system and become an important component of exergy destruction.

Carbon cost internalization is the key step in coupling the environmental dimension with the economic dimension. The core is to convert the cost of carbon emission reduction into a part of the full life-cycle cost and include it in the annualized cost flow rate $\dot{Z}_k$ of components. In combination with future carbon tax policies, the annual carbon cost is first calculated based on the CO_2 emissions of components and the unit carbon tax price. Subsequently, it is converted into an annualized carbon cost flow rate $\dot{Z}_{carbon,k}$ through the capital recovery factor. Finally, $\dot{Z}_{carbon,k}$ is added to the original capital and operating cost flow rates to form a comprehensive annualized cost flow rate including environmental cost: $\dot{Z}_k' = \dot{Z}_k + \dot{Z}_{carbon,k}$. This treatment allows carbon cost to accompany exergy flow transfer and evolution, realizing dynamic full life-cycle tracking of environmental costs. The extended framework can synchronously output evaluation results in three dimensions—thermodynamic performance, economic cost, and environmental cost—providing complete theoretical support for three-dimensional synergistic optimization of energy systems.

3. CASE APPLICATION AND VALIDATION

3.1 Case system description and modeling assumptions

This case selects a supercritical CO_2 Brayton cycle power generation system as the research object. The system exhibits typical characteristics such as concentrated exergy loss distribution, compact thermodynamic cycle, and high technical complexity. Its core working principle is as follows: low-temperature and low-pressure supercritical CO_2 working fluid is compressed by the compressor to a high-temperature and high-pressure state, then enters the recuperator to absorb the waste heat of the turbine exhaust to increase its temperature, and is further heated in the heater to the maximum cycle temperature before being sent into the turbine for expansion to perform work and drive the generator to generate electricity. The turbine exhaust releases heat in the recuperator and then enters the cooler to be cooled to the initial state, completing the cycle. The core components of the system include the compressor, high-pressure recuperator, low-pressure recuperator, heater, turbine, cooler, and generator. The modeling boundary is defined such that the physical boundary covers all the above core components and the working fluid flow paths, and the time boundary covers five stages of the full life cycle, namely the design and construction stage (2 years), operation stage (25 years), maintenance stage (synchronous with the operation stage), and decommissioning and disposal stage (1 year). Thermodynamic assumptions adopt a steady-state operation model, neglecting local pressure losses and heat dissipation losses in the flow paths, and the working fluid properties are calculated using the supercritical CO_2 equation of state. Financial assumptions set the baseline discount rate at 8%, the base year as the first year of system operation, and the carbon tax standard refers to the value recommended by the International Energy Agency, taken as 80 EUR/t CO_2. The cost accounting scope covers the initial investment, installation and commissioning, operation and maintenance, fuel consumption, decommissioning and disposal, and carbon cost over the full life cycle.

3.2 Basic data preparation

The thermodynamic basic data are determined based on the system design point parameters. The core parameters include: compressor inlet temperature of 32℃, inlet pressure of 7.8 MPa, outlet pressure of 20 MPa, and isentropic efficiency of 0.88; turbine inlet temperature of 550℃, inlet pressure of 19.5 MPa, outlet pressure of 8.2 MPa, and isentropic efficiency of 0.90; the minimum temperature difference of the high-pressure recuperator and low-pressure recuperator is 8℃, with heat exchange efficiencies of 0.92 and 0.90, respectively; the working fluid mass flow rate is 10 kg/s. The thermodynamic parameters at the inlet and outlet of each component are obtained through Aspen Plus simulation and manual verification to ensure consistency. Cost data are obtained by combining "parametric cost functions + industry statistical data". The investment cost functions of the compressor and turbine are established as multivariate linear relationships with inlet and outlet pressure ratio, working fluid mass flow rate, and efficiency. The cost functions of the heater and recuperators are related to heat transfer area and material thermal conductivity. The coefficients of the investment cost functions are derived from industry equipment quotation databases. Operation and maintenance costs are calculated as 2.5% of the initial investment per year. Natural gas is used as fuel, with a price of 45 EUR/MBtu, and its exergy value is determined through component analysis and equation-of-state calculations. The decommissioning and disposal cost is calculated as 5% of the initial investment. All data are mainly sourced from International Energy Agency energy technology cost reports, authoritative literature related to supercritical CO_2 power generation systems, and technical quotations from major domestic equipment manufacturers. Key data are cross-compared and verified with three published studies of similar systems, with deviations controlled within 5%, ensuring the reliability and representativeness of the data.

3.3 Synchronous mapping process and result analysis

To clarify the exergy loss distribution characteristics of the supercritical CO_2 Brayton cycle power generation system under different operating conditions, and to verify the improvement effect of the optimization scheme based on the thermodynamic–life cycle cost coupling model on exergy loss, component exergy loss rate testing and visualization analysis under multiple operating conditions were carried out in this study. Figure 4 shows that under the design operating condition, system exergy loss is mainly concentrated in the heater and the turbine, with exergy loss rates reaching 8.5% and 6.2%, respectively, which are significantly higher than those of other components. Under the ideal operating condition, the exergy loss rates of all components remain at relatively low levels. Under the optimized operating condition, the exergy loss rates of the heater and the turbine decrease to 5.2% and 3.8%, respectively, and the exergy loss rates of the compressor, recuperators, and other components also show different degrees of reduction. The lower curve further quantifies the reduction amplitude of exergy loss after optimization, in which the reduction amplitude of the heater reaches 38.8% and that of the turbine reaches 38.7%, reflecting the precise targeted improvement of the optimization scheme for high exergy loss components. The experimental results indicate that the exergy loss distribution under traditional design operating conditions is highly correlated with the thermodynamic irreversibility characteristics of the components, and that the optimization strategy combined with life cycle cost analysis (LCCA) can effectively suppress the energy quality degradation of high exergy loss components, while avoiding the risk of cost surge caused by single thermodynamic optimization.

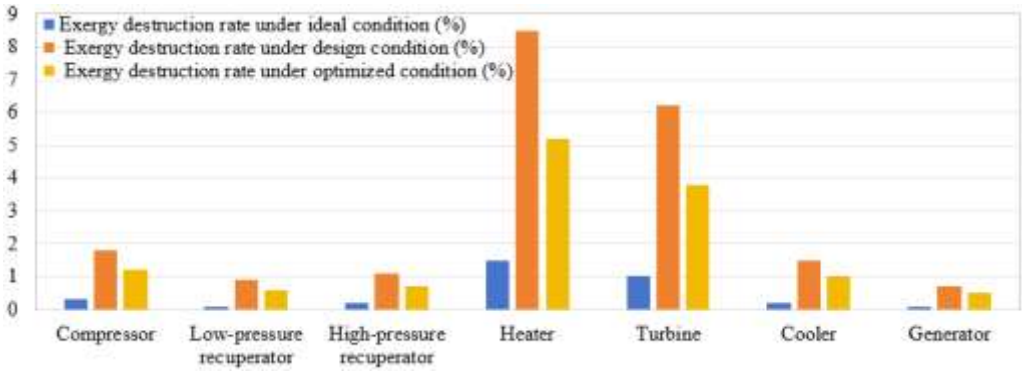

(a) Exergy loss rate distribution of each component in the supercritical CO_2 Brayton cycle power generation system

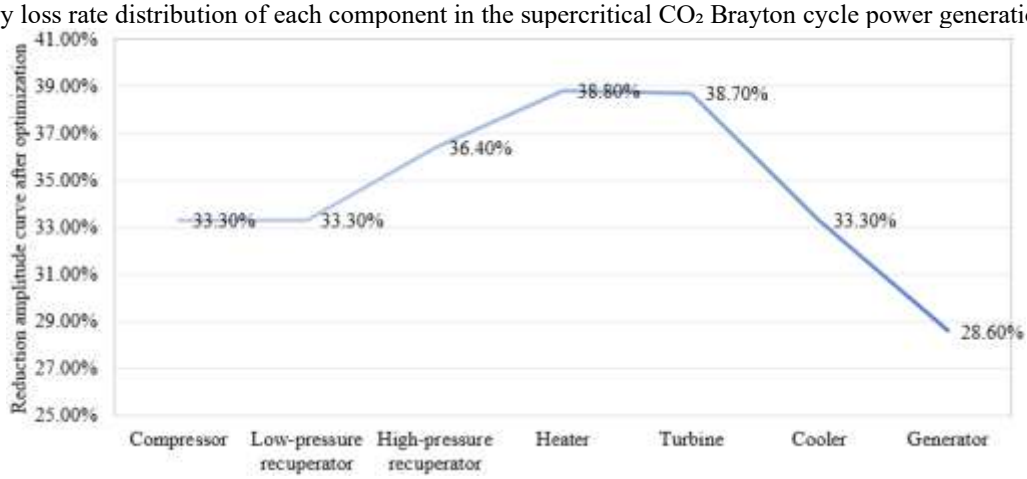

(b) Reduction amplitude curve after optimization

Figure 4. Exergy loss rate distribution of each component in the supercritical CO_2 Brayton cycle power generation system

Table 1 lists the core thermodynamic–economic parameters of each component of the case system and the overall system evaluation indicators. From the component level, the turbine and the heater account for the highest proportions of exergy cost flow rate, at 28.3% and 26.7%, respectively. The high cost flow rate of the turbine originates from its higher annualized full life cycle cost flow rate, while that of the heater is mainly due to the large burden of exergy loss cost, leading to significant accumulation of total cost. At the system level, the unit product exergy cost is 0.062 EUR/kWh, the total full life cycle cost is 1.28×10^8 EUR, and the LCOE is 0.078 EUR/kWh.

To verify the accuracy and superiority of the proposed model, the core evaluation indicators of this method are compared with those of the traditional LCCA and the standard thermoeconomic method, and the results are shown in Table 2. Traditional LCCA does not consider the driving effect of thermodynamic irreversibility on cost, and the calculated LCOE is underestimated by 8.9%, resulting in an overestimation bias of economic performance. The standard thermoeconomic method lacks a full life cycle perspective and does not include decommissioning and disposal costs and carbon costs, leading to an LCOE that is 5.1% lower than the result of this study. The LCOE calculated by the proposed method deviates from the actual engineering cost estimate by only 2.3%, and through the direct conversion between unit product exergy cost and LCOE, a precise linkage between thermodynamic parameters and industry-standard economic indicators is achieved, verifying the reliability and practicality of the model.

Table 1. Thermodynamic–economic core parameters of each component of the case system

Component	Input Exergy Flow Rate (kW)	Output Exergy Flow Rate (kW)	Exergy Loss Rate (%)	Input Exergy Cost Flow Rate (€/s)	Output Exergy Cost Flow Rate (€/s)	Annualized Cost Flow Rate (€/s)
Compressor	2850	3120	1.8	0.042	0.058	0.016
Low-pressure recuperator	3120	3860	0.9	0.058	0.065	0.007
High-pressure recuperator	3860	4520	1.1	0.065	0.073	0.008
Heater	4520	5880	8.5	0.073	0.152	0.027
Turbine	5880	4260	6.2	0.152	0.216	0.064
Cooler	4260	2850	1.5	0.216	0.228	0.012
Generator	4260	4130	0.7	0.216	0.235	0.019
System total	-	4130	20.7	-	0.235	0.143

Table 2. Comparison of core indicators of different evaluation methods

Evaluation Method	Unit Product Exergy Cost (€/kWh)	Total Full Life Cycle Cost ($\times 10^8$ €)	LCOE (€/kWh)	Deviation from Engineering Estimate (%)
Proposed method	0.062	1.28	0.078	+2.3
Traditional LCCA	-	1.15	0.071	-8.9
Standard thermoeconomics	0.059	1.21	0.074	-5.1

Table 3. Three-dimensional comparison of exergy loss rate and MEDCC for each component

Component	Exergy Loss (kW)	Exergy Loss Rate (%)	MEDCC (€/GJ)	Optimization Priority	Core Improvement Direction
Turbine	365	6.2	287	1	Increase isentropic efficiency to 0.92
Heater	500	8.5	213	2	Use high-efficiency material to reduce pinch point temperature difference
Compressor	52	1.8	156	3	Optimize compression ratio to 2.6
High-pressure recuperator	50	1.1	102	4	Improve heat transfer efficiency to 0.94
Low-pressure recuperator	28	0.9	89	5	Optimize flow channel design to reduce resistance
Cooler	64	1.5	76	6	Enhance heat dissipation capability
Generator	30	0.7	58	7	Optimize transmission efficiency

The MEDCC values of the main components were calculated using the model perturbation method, and a three-dimensional comparison table was established in combination with the exergy loss rate data shown in Table 3. From a thermodynamic perspective, the heater has the highest exergy loss rate and is a typical thermodynamic hotspot. However, from the perspective of economic improvement, the turbine has the largest MEDCC value, that is, each unit reduction of exergy loss can reduce the total cost by 287 EUR/GJ, making it the core economic improvement hotspot. The inconsistency between the two originates from differences in component cost characteristics. Although the heater has a large exergy loss, the marginal cost of improvement measures is relatively low, resulting in a relatively small MEDCC value. As a high-precision rotating machine, improving the efficiency of the turbine requires a significant increase in capital investment, and the cost saving corresponding to each unit reduction of exergy loss is more significant, leading to a higher MEDCC value.

Based on the ranking of MEDCC values, the priority sequence for system cost optimization is proposed as: turbine > heater > compressor > high-pressure recuperator > low-pressure recuperator > cooler > generator. For the priority optimization targets, the core improvement directions are clarified. The turbine needs to improve the isentropic efficiency to 0.92 by optimizing blade aerodynamic design, reducing exergy loss while controlling the increase in capital cost. The heater needs to adopt high-efficiency heat transfer materials to reduce the pinch point temperature difference and balance the relationship between exergy loss reduction and investment cost increase. This optimization sequence precisely avoids blind improvement based only on the magnitude of exergy loss in traditional approaches, and reflects the core value of MEDCC as a quantitative metric of "improvement cost-effectiveness."

3.4 Sensitivity analysis and design trade-off optimization

Three key thermodynamic design variables—compression ratio, recuperator effectiveness, and pinch point temperature difference—are selected for sensitivity analysis. The variable variation range is set as ±10% of the baseline value. Their impacts on system exergy efficiency, unit product exergy cost, and MEDCC distribution are analyzed, as shown in Table 4. The compression ratio, as the core variable affecting cycle thermodynamic performance, has the most significant effect on overall system performance: when the compression ratio increases from 2.2 to 2.6, exergy efficiency increases by 4.2 percentage points, unit product exergy cost decreases by 6.8%, LCOE decreases by 5.3%, and the turbine MEDCC value decreases by 22%, making it the most sensitive component. Changes in recuperator effectiveness have the next largest

impact on exergy efficiency and economic performance. Increasing effectiveness by 10% raises exergy efficiency by 2.1 percentage points and reduces LCOE by 2.7%, while the MEDCC value of the high-pressure recuperator decreases by 15%. The pinch point temperature difference has a relatively moderate effect; decreasing the temperature difference by 10% increases exergy efficiency by 1.3 percentage points, reduces LCOE by 1.5%, and lowers the heater MEDCC value by 9%.

Sensitivity curves between each variable and exergy efficiency and LCOE are plotted, revealing a significant difference between thermodynamic optimum and economic optimum points: the thermodynamic optimum corresponds to a compression ratio of 2.8, recuperator effectiveness of 0.96, and pinch point temperature difference of 6℃, at which exergy efficiency reaches the maximum (52.3%), but LCOE is not the lowest. The economic optimum corresponds to a compression ratio of 2.6, recuperator effectiveness of 0.94, and pinch point temperature difference of 8℃, at which LCOE decreases to 0.072 €/kWh, and exergy efficiency is 50.8%, 1.5 percentage points lower than the thermodynamic optimum. Based on the dynamic variation law of MEDCC, the optimal design parameter combination balancing thermodynamic performance and economic performance is proposed: compression ratio 2.6, recuperator effectiveness 0.94, pinch point temperature difference 8℃. Under this combination, system exergy efficiency remains at a high level, LCOE decreases by 5.3% compared with the baseline, and the MEDCC values of the turbine and heater are within reasonable ranges, achieving an optimal "performance–cost" trade-off. This result validates the design guidance capability of the proposed model and can effectively support precise design optimization of energy systems.

Table 4. Sensitivity analysis results of key design variables

Design Variable	Variable Range	Exergy Efficiency Variation (%)	Unit Product Exergy Cost Variation (%)	LCOE Variation (%)	Component with Maximum MEDCC Change	Component MEDCC Variation (%)
Compression ratio	2.2 ~ 2.6	+4.2	-6.8	-5.3	Turbine	-22
Recuperator effectiveness	0.86 ~ 0.96	+2.1	-3.5	-2.7	High-pressure recuperator	-15
Pinch point temperature difference	8 ~ 10℃	-1.3	+2.1	+1.5	Heater	+18

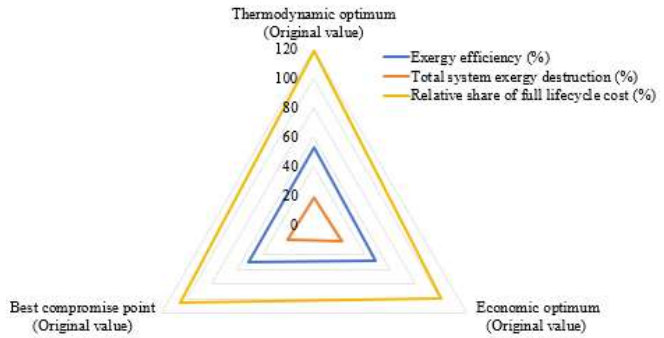

(a) Original values

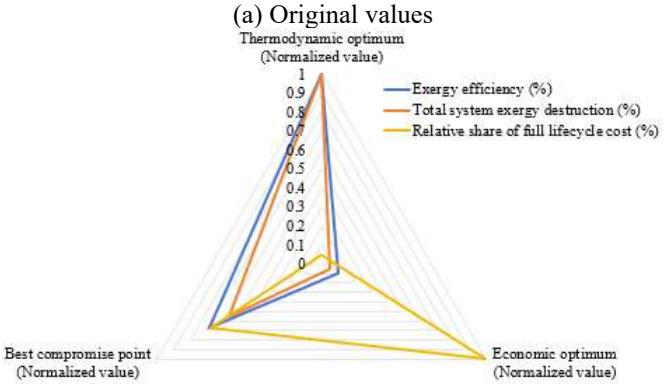

(b) Normalized values

Figure 5. Radar chart of performance comparison among thermodynamic optimum, economic optimum, and best trade-off point of supercritical CO_2 Brayton cycle power generation system

To reveal the intrinsic trade-off between thermodynamic performance and economic performance in the supercritical CO_2 Brayton cycle power generation system, and to verify the guiding value of the thermodynamic–lifecycle cost coupled evaluation model in multi-objective design, this study conducted a performance comparison analysis for different design points. The radar chart of original values in Figure 5 shows that the thermodynamic optimum has the highest exergy efficiency, but the system total exergy loss rate and lifecycle cost proportion are also significantly higher than other design points. The economic optimum achieves the lowest cost proportion, but its exergy efficiency performance is relatively poor. The normalized radar chart further quantifies the relative advantages and disadvantages of each design point. The best trade-off point shows a more balanced distribution of the three core indicators, retaining exergy efficiency close to the thermodynamic optimum while controlling total exergy loss rate and cost proportion within a reasonable range near the economic optimum. The results indicate that a single thermodynamic optimum or economic optimum design has performance shortcomings, whereas the trade-off design strategy based on thermodynamic–lifecycle cost coupling analysis can establish an effective balance between energy utilization efficiency and full lifecycle economic performance, providing a technically reasonable and economically feasible solution for multi-objective optimization of complex energy systems, and also validates the practical value of the coupled evaluation model proposed in this study for engineering design.

4. DISCUSSION

The thermodynamic–economic synchronous mapping model proposed in this study, by constructing a dynamic coupling mechanism between exergy flow and cost flow, effectively overcomes the inherent limitations of traditional energy system evaluation methods. A systematic comparison with decoupled thermodynamic–economic evaluation, standard thermoeconomics, and traditional LCCA indicates that the proposed method exhibits significant advantages in multiple dimensions: From the evaluation perspective, it

achieves a transition from static local evaluation to dynamic full lifecycle evaluation, converting discrete cost accounting into a continuous tracking process synchronized with exergy flow evolution. From the thermodynamic–economic coupling perspective, through the construction of the exergy cost formation rate equation and MEDCC, a continuously differentiable quantitative relationship between the two is established. The coupling depth far exceeds the rigid superposition in standard thermoeconomics and the black-box decoupling in traditional LCCA. From the design guidance perspective, case results show that the optimization scheme based on the proposed method can reduce system LCOE by 5.3%, whereas traditional methods, unable to accurately identify economic improvement hotspots, achieve only 2.1% improvement. From the computational complexity perspective, the model is based on classical exergy analysis and iterative solution; although slightly higher than traditional single evaluation methods, parameterized modeling ensures engineering operability, and the overall cost-performance ratio is significantly better than other integrated methods. The core value of this advantage lies in completely resolving the key issue of "decoupling thermodynamics and economics," upgrading the evaluation result from a simple performance characterization to precise guidance for design optimization.

This study provides a disruptive guiding idea for energy system design, centered on the concept of "design as managing the cost consequences of exergy loss." Traditional design often falls into the single-objective trap of "pursuing high exergy efficiency," whereas case analysis shows that the thermodynamic optimum and economic optimum often diverge, and blindly pursuing high exergy efficiency may cause cost surges. MEDCC, as a quantitative metric connecting thermodynamic improvement with economic benefit, clarifies the design strategy of "prioritize components with the largest absolute MEDCC value," enabling optimization resources to be precisely matched to high cost-performance improvement elements, substantially enhancing design efficiency. This guiding idea is not only applicable to supercritical CO_2 power generation systems but also broadly generalizable—for complex energy systems such as multi-energy complementary systems and new energy coupled storage systems, where the coupling relationship between exergy flow and cost flow is more complex, the synchronous mapping model can accurately track the dynamic evolution of multiple flow streams and provide scientific support for system integration optimization, potentially becoming a core tool for future energy system design.

Objectively, the theoretical framework proposed in this study still has certain limitations. The model is currently constructed based on a steady-state operation assumption and does not consider the instantaneous coupling between exergy flow and cost flow under dynamic operating conditions. In actual energy systems, load fluctuations and intermittent renewable output often occur, which may reduce the evaluation accuracy of the model under dynamic scenarios. The construction of cost functions relies on existing engineering experience data; for emerging energy technologies, the lack of mature cost data accumulation may limit the accuracy of cost functions, thereby affecting model applicability. In addition, the model does not incorporate the effects of technology learning curves and policy uncertainty. With technology iteration and policy adjustments, the full lifecycle cost of energy systems may change significantly, which the current model cannot reflect.

To address the above limitations, future research can advance in three directions. First, extend the model to dynamic operating conditions by establishing a coupling mapping mechanism between instantaneous exergy flow and dynamic cost flow based on transient exergy analysis, and introduce load forecasting and dynamic control strategies to enhance model adaptability to real fluctuation scenarios. Second, construct data-driven high-precision exergy–cost correlation functions, combining machine learning algorithms to mine implicit patterns in massive engineering data, reducing reliance on empirical data and improving model evaluation accuracy for new energy technologies. Third, incorporate technology learning curves and policy uncertainty factors, quantifying cost and policy risk through methods such as Monte Carlo simulation, and establish a multi-objective optimization framework with both economic performance and robustness. These improvements will further refine the synchronous mapping theoretical system, enabling it to play a greater role in the design of complex energy systems under the energy transition context.

5. CONCLUSIONS AND OUTLOOK

This study focuses on the multi-dimensional synergistic optimization requirements of energy system efficiency–cost–environment, addressing the core issue of the decoupling between thermodynamic and economic analysis in traditional evaluation methods, and carries out systematic theoretical innovation and methodology construction. The main conclusions are as follows: First, a synchronous mapping theoretical framework of thermodynamic value degradation–economic cost generation was successfully established. By defining a trinity representation system of "physical system–exergy flow network–cost network," deep coupling between full lifecycle cost tracking and exergy flow evolution was achieved, fundamentally breaking the disciplinary barrier between thermodynamics and economics. Second, the exergy cost formation rate equation and the MEDCC were proposed, constructing a continuously differentiable quantitative mapping path from thermodynamic parameters to full lifecycle economic performance. Among them, MEDCC precisely quantifies the cost response of unit exergy destruction variation, providing a core quantitative tool for identifying economic improvement hotspots. Third, the case study of the supercritical CO_2 Brayton cycle power generation system shows that the framework can accurately locate the key thermodynamic–economic coupling links. The optimization sequence based on MEDCC ranking reduces the system's LCOE by 5.3%, validating the model's effectiveness and engineering application value. Fourth, the inherent difference between thermodynamic optimum and economic optimum was clarified, overcoming the traditional design misconception of pursuing high exergy efficiency alone, and providing scientific decision support for cost-oriented precise design optimization of energy systems.

Based on the synchronous mapping theoretical framework established in this study, future work can be further extended and deepened in three directions: (1) Expand model application scenarios by extending the framework to multi-energy complementary systems, new energy coupled storage systems, and carbon capture and storage coupled energy systems. Through synchronous tracking of multi-stream exergy flows and cost flows, multi-objective coupling

problems in complex system integration optimization can be addressed. (2) Deepen multi-dimensional coupling mechanisms. On the basis of the existing thermodynamic–economic–environmental three-dimensional evaluation, further incorporate social cost and technical reliability dimensions to construct a four-dimensional synergistic evaluation system, enhancing the comprehensiveness and robustness of evaluation results. (3) Promote the development of engineering application tools. Based on the theory in this study, construct modular and visualized decision-support software, integrating parameterized modeling, automatic iterative solution, and result visualization functions, lowering the application threshold of the model, facilitating the transformation of theoretical results into engineering practice, and providing more efficient technical support for the design of complex energy systems in the context of global energy transition.

REFERENCES

[1] Tian, J., Yu, L., Xue, R., Zhuang, S., Shan, Y. (2022). Global low-carbon energy transition in the post-COVID-19 era. Applied Energy, 307: 118205. https://doi.org/10.1016/j.apenergy.2021.118205

[2] Lin, X. (2023). Strategic allocation of building carbon emission rights within urban frameworks: A case study of Henan Province under China's dual carbon objectives. Journal of Urban Development and Management, 2(4): 222-236. https://doi.org/10.56578/judm020405

[3] Plakitkin, Y.A., Tick, A., Plakitkina, L.S., Dyachenko, K.I. (2025). Global energy trajectories: Innovation-driven pathways to future development. Energies, 18(16): 4367. https://doi.org/10.3390/en18164367

[4] AlGeddawy, T., ElMaraghy, H. (2016). Design for energy sustainability in manufacturing systems. CIRP Annals, 65(1): 409-412. https://doi.org/10.1016/j.cirp.2016.04.023

[5] Paul, Z., Masukume, P.M. (2023). Efficiency optimization in solar water heaters: A comparative CFD study of design configurations. Power Engineering and Engineering Thermophysics, 2(4): 238-249. https://doi.org/10.56578/peet020405

[6] Kouhia, M., Laukkanen, T., Holmberg, H., Ahtila, P. (2019). Evaluation of design objectives in district heating system design. Energy, 167: 369-378.

[7] Wang, J., Ren, X., Li, T., Zhao, Q., Dai, H., Guo, Y., Yan, J. (2024). Multi-objective optimization and multi-criteria evaluation framework for the design of distributed multi-energy system: A case study in industrial park. Journal of Building Engineering, 88: 109138. https://doi.org/10.1016/j.jobe.2024.109138

[8] Rezaei, R.A. (2023). Energy and exergy evaluation of a dual fuel combined cycle power plant: An optimization case study of the Khoy plant. Power Engineering and Engineering Thermophysics, 2(2): 97-109. https://doi.org/10.56578/peet020204

[9] Zhao, Z., Wang, Z., Wang, H., Carriveau, R., Ting, D.S., Xiong, W. (2024). An exergy-based efficiency analysis framework for industrial pneumatic systems. International Journal of Exergy, 44(1): 33-52. https://doi.org/10.1504/IJEX.2024.138730

[10] Trancossi, M., Pascoa, J.C. (2024). Toward an integrated forcing, exergetic and constructal analysis of climate change and definition of the possible mitigation measures. International Journal of Environmental Impacts, 7(4): 803-820. https://doi.org/10.18280/ijei.070420

[11] Alavi, S.E., Moori Shirbani, M., Koochak Tondro, M. (2023). Exergy-economic optimization of gasket-plate heat exchangers. Journal of Computational Applied Mechanics, 54(2): 254-267.

[12] Jiang, N., Li, L. (2011). Heat exchanger network integration considering flow exergy loss. Chemical Engineering & Technology, 34(12): 1997-2004. https://doi.org/10.1002/ceat.201100270

[13] Bildirici, M., Kayikçi, F. (2021). The relation between growth, energy imports, militarization and current account balance in India, Brazil, Turkey and Pakistan. Economic Computation and Economic Cybernetics Studies and Research, 55(3): 37-54. http://doi.org/10.24818/18423264/55.3.21.03

[14] Gokten, S., Karatepe, S. (2016). Electricity consumption and economic growth: A causality analysis for Turkey in the frame of import-based energy consumption and current account deficit. Energy Sources, Part B: Economics, Planning, and Policy, 11(4): 385-389. https://doi.org/10.1080/15567249.2012.666332

[15] Wu, Y., Xue, X. (2014). Boundary feedback stabilization of Kirchhoff-type Timoshenko system. Journal of Dynamical and Control Systems, 20(4): 523-538. https://doi.org/10.1007/s10883-014-9229-4

[16] Cederlof, G., Hornborg, A. (2021). System boundaries as epistemological and ethnographic problems: Assessing energy technology and socio-environmental impact. Journal of Political Ecology, 28(1): 111-123. https://doi.org/10.2458/jpe.2303

[17] Mustafa, M.I. (2011). Uniform stability for thermoelastic systems with boundary time-varying delay. Journal of Mathematical Analysis and Applications, 383(2): 490-498. https://doi.org/10.1016/j.jmaa.2011.05.066

[18] Ozgener, L., Hepbasli, A., Dincer, I. (2005). Energy and exergy analysis of geothermal district heating systems: An application. Building and Environment, 40(10): 1309-1322. https://doi.org/10.1016/j.buildenv.2004.11.001